Olefin Insertion into the Rhodium−Hydrogen Bond as the Step Determining the Regioselectivity of Rhodium-Catalyzed Hydroformylation of Vinyl Substrates: Comparison between Theoretical and Experimental Results

Giuliano Alagona,*[,†,‡] Caterina Ghio,[†,§] Raffaello Lazzaroni,[‖] and Roberta Settambolo[†,⊥]

Institute of Quantum Chemistry and Molecular Energetics, CNR, Via Moruzzi 1, I-56124 Pisa, Italy, and the Department of Chemistry and Industrial Chemistry, University of Pisa, Via Risorgimento 35, I-56126 Pisa, Italy

Received August 8, 2001

A comparison between experimental and theoretical data on regioselectivity concerning the hydroformylation of several vinyl substrates (propene, 2-methylpropene, 1-hexene, 3,3-dimethylbutene, fluoroethene, 3,3,3-trifluoropropene, vinylmethylether, allylmethylether, styrene) with unmodified rhodium catalysts is reported. Various H−Rh(CO)$_3$–olefin complexes are examined at the B3P86/3-21G or /6-31G* level (LANL2DZ for Rh) and compared to the adducts with modified catalysts, such as H−RhPH$_3$(CO)$_2$. The computed geometries are in satisfactory agreement with the X-ray ones. The activation energies for the alkyl rhodium intermediate formation, computed at either level along the pathways to branched or linear aldehydes, allow one to predict the regioselectivity ratios, since they are in very good agreement with the experimental ones evaluated for the isomeric aldehydes.

Downloaded by CARLI CONSORTIUM on June 29, 2009
Published on November 7, 2001 on http://pubs.acs.org | doi: 10.1021/om010721m

Introduction

Hydroformylation of alkenes, the most important catalytic process for the production of aldehydes,[1] discovered about 60 years ago,[2] is yet the object of extensive investigations from both the experimental[1,3] and theoretical[4] viewpoints. A number of transition metal complexes are used as catalysts, though the most common are low-valent cobalt and rhodium[3a,5] complexes. The main goal of the rhodium-catalyzed hydroformylation of unsaturated substrates, especially of the vinyl ones, concerns the control of the reaction regioselectivity, i.e., of the regioisomeric ratio, branched to linear (**b**:**l**), between the aldehydes produced, as displayed in Scheme 1.

Scheme 1

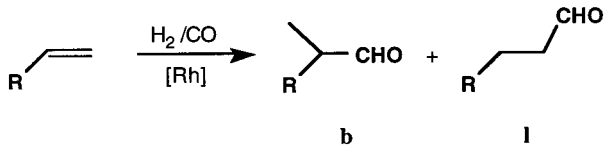

The substrate structure and properties, the reaction parameters (*P*, *T*, concentration), and the nature of the catalyst (unmodified or modified with phosphorus ligands) are the main factors that affect the regioselectivity.

Several, though sometimes conflicting, hypotheses have been put forward to rationalize the regioselectivity of the vinyl substrate hydroformylation,[6] such as coordination of the CO group to the catalytic system for unsaturated ethers,[6b] the inductive effect of substituents to the double bond in the case of trifluoropropene[6c] or substituted styrenes,[6d] and the kinetic lability of acyl complexes, saturated or not, in the case of styrenes[6e] and vinyl esters.[6f] Recently, however, careful deuterioformylation experiments with unmodified ($Rh_4(CO)_{12}$) rhodium precatalysts, carried out on vinyl substrates of different structures at partial conversion under mild conditions, clearly demonstrated that the insertion of the olefin into the Rh−H bond is not reversible.[7]

† Institute of Quantum Chemistry and Molecular Energetics.
‡ E-mail: G.Alagona@icqem.pi.cnr.it. Web site: http://www.icqem-.pi.cnr.it/kitty/alagiEn.
§ E-mail: C.Ghio@icqem.pi.cnr.it. Web site: http://www.icqem.pi.cnr.it/kitty/kittyEn.
‖ University of Pisa. E-mail: Lazza@dcci.unipi.it. Web site: http://www.dcci.unipi.it.
⊥ E-mail: R.Settambolo@icqem.pi.cnr.it. Web site: http://www.icqem.pi.cnr.it.

(1) (a) Cornils, B.; Herrmann, W. A. *Applied Homogeneous Catalysis with Organometallic Compounds*; VCH−Wiley: New York, 1996; Vol. 1, pp 3−25. (b) Papadogianakis, G.; Sheldon, R. A. *New J. Chem.* **1996**, *20*, 175.

(2) Roelen, O. (Ruhrchemie AG). D. B. P. 849 458, 1938; *Chem. Zentr.* **1953**, 927.

(3) (a) Süss-Fink, G.; Meister, G. *Adv. Organomet. Chem.* **1993**, *35*, 41. (b) Ungváry, F. *Coord. Chem. Rev.* **1997**, *167*, 233. (c) Ungváry, F. *Coord. Chem. Rev.* **1998**, *170*, 245. (d) Ungváry, F. *Coord. Chem. Rev.* **1999**, *188*, 263.

(4) Torrent, M.; Solà, M.; Frenking, G. *Chem. Rev.* **2000**, 100, 439 and refs. therein.

(5) (a) Wender, I.; Pino, P. *Organic Syntheses via Metal Carbonyls*; Wiley-Interscience: New York, 1977, vol. 2. (b) Falbe, J. *New Syntheses with Carbon Monoxide*; Springer: Berlin, 1980.

(6) (a) Feng, J.; Garland, M. *Organometallics* **1999**, *18*, 417. (b) Matsumoto, M.; Tamura, M. *J. Mol. Catal.* **1982**, *16*, 195. (c) Fuchikami, T.; Ojima, I. *J. Am. Chem. Soc.* **1982**, *104*, 3527. (d) Hayashi, T.; Tanaka, M.; Ogata, I. *J. Mol. Catal.* **1981**, *13*, 323. (e) Brown, J. M.; Kent, A. G. *J. Chem. Soc. Chem. Commun.* **1982**, 723. (f) Abatjoglou, A. G.; Bryant, D. R. Award Symposium on Catalysis for Chemicals and Fuels, Atlanta, March 29-April 3, 1981.

10.1021/om010721m CCC: $20.00 © 2001 American Chemical Society
Publication on Web 11/07/2001

Scheme 2

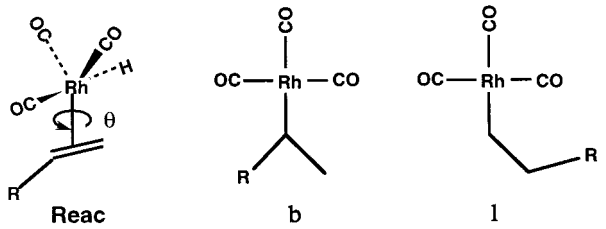

Therefore, the regioselectivity of the aldehydes originates during the formation of isomeric alkylrhodium intermediates. Analogous results have been obtained for styrene deuterioformylation[8a] carried out in the presence of rhodium catalysts modified with chiral phosphine BINAPHOS,[8b] as well as for the alkyl olefin deuterioformylation performed with chelating diphosphine rhodium catalysts.[8c,d] Thus, the olefin insertion into the Rh−H bond is nowadays regarded as the crucial step determining the regioselectivity of the whole process.

Since the isomeric alkylmetal intermediates are very reactive under typical hydroformylation conditions, no direct experimental evidence of their formation is available, and thence, an experimental determination of their relative concentrations is not allowed. Concerning this reaction step, it should be noted that the structure of the final product (the square-planar isomeric alkyl) is well defined, whereas there is still uncertainty concerning the pentacoordinated starting complex ($H-Rh(CO)_3$•olefin).[4,9] One of its possible roughly trigonal-bipyramidal (TBP) structures is shown in Scheme 2 (Reac).

Therefore, an accurate theoretical investigation of the kinetic and thermodynamics aspects of the aforementioned step is interesting and may in principle be carried out. The use of unmodified rhodium precatalysts such as $Rh_4(CO)_{12}$, which under reaction conditions gives rise to $H-Rh(CO)_3$, in equilibrium with $H-Rh(CO)_4$, permits a direct comparison between theoretical and experimental results making use of the same catalyst. In addition, also the number of isomers to consider is lower, while the absence of phosphines sharply reduces the computational complexity.

Most of the experimental investigations on hydroformylation have been carried out until now in the presence of phosphine-modified catalysts;[5,10] conversely, several reports on the oxo reactions of unsaturated substrates performed with unmodified rhodium systems have been published.[11] To make a reliable and consistent comparison between experimental (related to aldehydes) and theoretical (related to alkyl species) regioselectivity values, a set of experiments on a wide series of vinyl compounds has been carried out under mild conditions (T = 25 °C, $P_{CO} = P_{H_2}$ = 40 atm). Hydrocarbon solvents (pentane, hexane, heptane), characterized by a low dielectric constant, were employed, in contrast with most of the investigations in the literature that are performed in more polar solvents such as benzene, dichloromethane, tetrahydrofuran, and ethanol.[5,8,10,11]

Ab initio MO studies on the hydroformylation of ethylene carried out with modified catalysts appeared in the literature,[12] but only few works have thus far discussed the hydroformylation regioselectivity from a theoretical point of view, using propene as the model olefin and pure density functional theory (DFT)[13] or hybrid DFT/molecular mechanical (QM/MM) methods.[14] In ref 14, MM was used to account for steric effects when bulky phosphines were considered. A tentative theoretical evaluation of regioselectivity for 1-hexene, carried out exclusively with MM methods, deriving the transition state geometries from a linear interpolation of the parameters along a symmetric reaction coordinate, was dismaying.[8d]

On the other hand, only unmodified cobalt−carbonyl species[13a] or catalytic precursors modified with phosphines[13b,14] have been considered in earlier calculations. With the exception of ref 14, the simplest phosphine, PH_3, was in general used as a ligand, though it has been pointed out that PH_3 is not suitable as a model of triphenylphosphine or other phosphines.[15]

To the best of our knowledge, no theoretical investigation on the reaction either of ethylene or higher olefins with unmodified rhodium catalysts has been reported thus far. Consequently, this is the first paper discussing the regioselectivity in the hydroformylation reaction performed with unmodified rhodium catalysts from a theoretical viewpoint.

Computational Details

The calculations were carried out in the density functional theory framework using the Becke's three-parameter hybrid exchange functional[16a] and the Perdew's P86 gradient-corrected correlation functional,[17] B3P86, at the 3-21G[18] and 6-31G*[19] levels, with the Gaussian98 system of programs.[20] The Becke's exchange functional[16b] was also used for comparison with a previous work.[13b] Effective core potentials, which include some relativistic effects for the electrons near the nucleus, have been used for Rh in the LANL2DZ[21] corresponding valence basis set, when not otherwise specified. A number

Downloaded by CARLI CONSORTIUM on June 29, 2009
Published on November 7, 2001 on http://pubs.acs.org | doi: 10.1021/om010721m

(7) Lazzaroni, R.; Uccello-Barretta, G.; Benetti, M. *Organometallics* **1989**, *8*, 2323.
(8) (a) Horiuchi, T.; Shirakawa, E.; Nozaki, K.; Takaya, H. *Organometallics* **1997**, *16*, 2981. (b) Nozaki, K.; Sakai, N.; Nanno, T.; Higashijima, T.; Mano, S.; Horiuchi, T.; Takaya, H. *J. Am. Chem. Soc.* **1997,** *119*, 4413, and refs. quoted therein. (c) Herrmann, W. A.; Kohlpaintner, C. W.; Herdtwck, E.; Kiprof, P. *Inorg. Chem.* **1991**, *30*, 4721. (d) Casey, C. P.; Petrovich, L. M. *J. Am. Chem. Soc.* **1995**, *117*, 6007.
(9) Pidun, U.; Frenking, G. *Chem. Eur. J.* **1998**, *4*, 522.
(10) (a) *Homogeneous Catalysis with Metal Phosphine Complexes*, Pignolet, L. H., Ed.; Plenum Press: New York, 1983. (b) Casey, C. P.; Paulsen, E. L.; Bettenmueller, E. W.; Proft, B. R.; Matter, B. A.; Powell, D. R. *J. Am. Chem. Soc.* **1999**, *119*, 11817. (c) Van Leeuwen, P. W. N. M.; Kamer, P. C. J.; Reek, J. N. H., *Pure Appl. Chem.* **1999**,*71*, 1443.
(11) Beller, M.; Cornils, B.; Frohning, C. D.; Kohlpaintner, C. W. *J. Mol. Catal. A: Chem.* **1995**, *104*, 17.
(12) (a) Koga, N.; Jin, S. Q.; Morokuma, K. *J. Am. Chem. Soc.* **1988**, *110*, 3417. (b) Matsubara, T.; Koga, N.; Ding, Y.; Musaev, D. G.; Morokuma, K. *Organometallics* **1997**, *16*, 1065.
(13) (a) Versluis, L.; Ziegler, T.; Fan, L. *Inorg. Chem.* **1990**, *29*, 4530. (b) Rocha, W. A.; De Almeida, W. B. *Int. J. Quantum Chem.* **2000**, *78*, 42.
(14) Gleich, D.; Schmid, R.; Herrmann, W. A. *Organometallics* **1998**, *17*, 4828.
(15) (a) Schmid, R.; Herrmann, W. A.; Frenking, G. *Organometallics* **1997**, *16*, 701. (b) González-Blanco, O.; Branchadell, V. *Organometallics* **1997**, *16*, 5556.
(16) (a) Becke, A. D. *J. Chem. Phys.* **1993**, *98*, 5648. (b) Becke, A. D. *Phys. Rev. A* **1988**, *38*, 3098.
(17) (a) Perdew, J. P. *Phys. Rev. B* **1986**, *33*, 8822. (b) Perdew, J. P. *Phys. Rev. B* **1986**, *34*, 7406.
(18) Binkley, J. S.; Pople, J. A.; Hehre, W. J. *J. Am. Chem. Soc.* **1980**, *102*, 939.
(19) (a) Ditchfield, R.; Hehre, W. J.; Pople, J. A. *J. Chem. Phys.* **1972**, *56*, 2257. (b) Hariharan, P. C.; Pople, J. A. *Theor. Chim. Acta* **1973**, *28*, 213.

Scheme 3

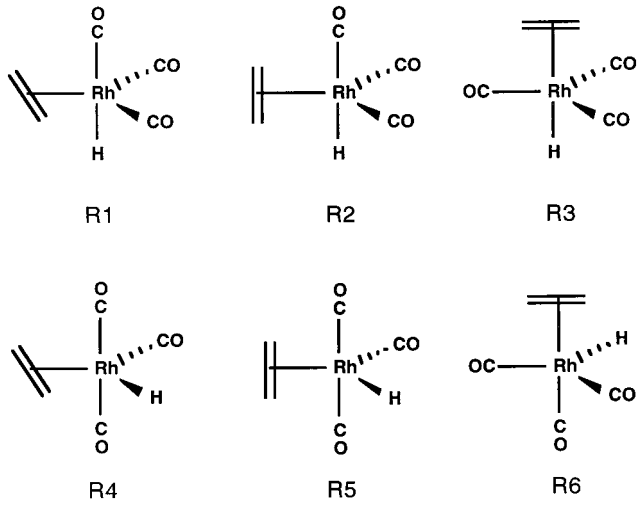

of calculations at different levels have, in fact, been carried out for comparison; reference is made to them, where appropriate. Zero point energies and thermal corrections have also been computed in the rigid rotator−harmonic oscillator approximation to obtain the free energies. The various terms are listed in Tables IS and IIS of the Supporting Information in order to allow the reader to combine them at will. Harmonic vibrational frequencies at the proper level were used throughout to confirm the nature of the stationary points found.

Results and Discussion

Stability of the Complexes. A preliminary scan of the potential energy surface (PES) for the olefin insertion was carried out at the B3P86/3-21G level, using ethene as a model olefin. A number of structures of the TBP starting complex were considered (shown in Scheme 3, with the bipyramid vertexes up or down and the trigonal base midway). The structure named R1 turned out to be the most stable, followed by R2 and R3 (respectively 4.85 and 5.02 kcal/mol higher in energy), whereas R4, R5, and R6 were not local minima and respectively plunged into R3, R1, and a structure in the region of the products.

Therefore, the structures featuring an equatorial H (i.e., located in the trigonal base of the bipyramid) seem to be unstable. On the contrary, when a phosphine group was present[12a] [The names in boldface (**1a**−**1g**) correspond to the structures of ref 12a.], the complexes related to R4 (**1d** ≡ **1e**) turned out to be equilibrium structures, while those related to R6 (**1f** ≡ **1g**) were defined as transition states (TS) "for rearrangement", with the exception of R5, not considered therein. Geometry optimizations at the TS actually need to be carried out to locate structures related to R4, R5, and R6 on the B3P86/3-21G LANL2DZ PES. Those structures, however, turn out to be square planar (SP), not TBP. The rearrangement occurs via a Berry pseudorotation mechanism, as shown earlier in phosphoranes:[22,23] the small barrier between the TBP and SP arrangements can easily be surmounted during the geometry optimization.

Table 1. Energetic Quantities at Various Levels (all making use of the 3-21G basis set) for TBP Complexes of Ethylene and Unmodified (upper part) or Modified (lower part) Rhodium Catalysts

ethene···H−Rh(CO)$_3$	B3P86 LANL2DZ	HF LANL1DZ	B3P86 LANL1DZ	MP2//MP2 LANL2DZ
R1	0[a]	0[b]	0[c]	0[d]
R2	4.85	4.09	3.16	7.84
TS (1−2)	12.50	17.57	6.97	15.04
P	−11.09	−12.15	−16.19	−1.51
ethene···HRh(CO)$_2$PH$_3$	B3P86 LANL2DZ	HF LANL1DZ	B3P86 LANL1DZ	HF ECP[e]
1a	0[f]	0[g]	0[h]	0
1a′	7.19	5.40	4.19	20.2
TS (1a−1a′)	15.76	20.35	8.28	21.2 (23.4)
2a	−10.37	−12.40	−15.18	−13.5

[a] Reference energy = −527.891 700 au. [b] Reference energy = −436.656 147 au; [c] Reference energy = −441.276 338 au. [d] Reference energy = −524.261 017 au [e] From ref 12a (reference energy not available), MP2//HF results in parentheses. [f] Reference energy = −756.689 100 au. [g] Reference energy = −665.256 472 au [h] Reference energy = −670.079 016 au

The structural difference between R1 and R2, which explains their energy gap, is the orientation of the olefin, as displayed in Scheme 3: in R1 the double bond is in the trigonal base of the bipyramid, whereas in R2 it is perpendicular to the base. The bond angle between the CO groups in the base thus raises from ∼120° in R1 to ∼140° in R2. On the contrary, in the presence of a phosphine group, at the HF/3-21G/ECP[21b] level with an STO-2G[24] description of the phosphine Hs, **1a′**, i.e., R2 with a phosphine in axial position, turned out to be 20.2 kcal/mol less stable than **1a** (R1 with a phosphine in axial position).[12a] This was a surprisingly large effect for a phosphine, which prompted us to carry out tentative calculations on modified catalysts as well.

The results obtained are compared in Table 1. The B3P86/3-21G LANL2DZ energy gap between the two structures **1a** and **1a′** turned out to be ∼7.2 kcal/mol. The calculations in ref 12a, however, were carried out at the HF level with a version of Gaussian (Gaussian82) probably not yet equipped with LANL2DZ. At the HF/3-21G LANL2DZ level, actually, very feeble interactions between ethene and the catalyst (either unmodified or modified) are found: the equilibrium distance of Rh and the ethene C atoms is, in fact, ∼4.3 Å for either arrangement of the double bond (parallel or perpendicular to the Rh−H bond). This is inconsistent with what was found at the B3P86 level, where the Rh···C separation is ∼2.4 Å for R1 and ∼2.7 Å for R2. Moreover,

Downloaded by CARLI CONSORTIUM on June 29, 2009
Published on November 7, 2001 on http://pubs.acs.org | doi: 10.1021/om010721m

(20) Frisch, M. J.; Trucks, G. W.; Schlegel, H. B.; Scuseria, G. E.; Robb, M. A.; Cheeseman, J. R.; Zakrzewski, V. G.; Montgomery, J. A.; Stratmann, R. E.; Burant, J. C.; Dapprich, S.; Millam, J. M.; Daniels, A. D.; Kudin, K. N.; Strain, M. C.; Farkas, O.; Tomasi, J.; Barone, V.; Cossi, M.; Cammi, R.; Mennucci, B.; Pomelli, C.; Adamo, C.; Clifford, S.; Ochterski, J.; Petersson, G. A.; Ayala, P. Y.; Cui, Q.; Morokuma, K.; Malick, D. K.; Rabuck, A. D.; Raghavachari, K.; Foresman, J. B.; Cioslowski, J.; Ortiz, J. V.; Stefanov, B. B.; Liu, G.; Liashenko, A.; Piskorz, P.; Komaromi, I.; Gomperts, R.; Martin, R. L.; Fox, D. J.; Keith, T.; Al-Laham, M. A.; Peng, C. Y.; Nanayakkara, A.; Gonzalez, C.; Challacombe, M.; Gill, P. M. W.; Johnson, B. G.; Chen, W.; Wong, M. W.; Andres, J. L.; Head-Gordon, M.; Replogle, E. S.; Pople, J. A. *Gaussian 98 (Revision A.7);* Gaussian, Inc.: Pittsburgh, PA, 1998.

(21) (a) Dunning, T. H., Jr.; Hay, P. J. In *Modern Theoretical Chemistry*, Schaefer, H. F., III, Ed.; Plenum: New York, 1976; pp. 1−28. (b) Hay, P. J.; Wadt, W. R. *J. Chem. Phys.* **1985**, *82*, 270. (c) Hay, P. J.; Wadt, W. R. *J. Chem. Phys.* **1985**, *82*, 299.

(22) Hoffmann, R.; Howell, J. M.; Muetterties, E. J. *J. Am. Chem. Soc.* **1972**, *94*, 3047.

(23) Altmann, J. A.; Yates, K.; Csizmadia, I. G. *J. Am. Chem. Soc.* **1976**, *98*, 1450.

(24) Hehre, W. J.; Stewart, R. F.; Pople, J. A. *J. Am. Chem. Soc.* **1969**, *51*, 2657.

Downloaded by CARLI CONSORTIUM on June 29, 2009
Published on November 7, 2001 on http://pubs.acs.org | doi: 10.1021/om010721m

$H-Rh(CO)_3$ turns out to be perfectly planar. Resorting to the HF/3-21G LANL1DZ level, sensible geometries of the complexes are obtained, but the energy difference between **1a** and **1a′** increases even less (∼5.4 kcal/mol). As a further control, we computed that energy gap with B3P86/3-21G LANL1DZ using either modified or unmodified catalysts, obtaining respectively ∼4.2 and ∼3.2 kcal/mol, though with analogous Rh···C separations (∼2.4 and ∼2.6 Å for **1a** and **1a′**, namely).

The effect of Møller−Plesset second order (MP2) correlation corrections[25] at the B3P86/3-21G optimized geometries as well as at the MP2/3-21G ones was also examined, with a particular interest in the reactant−product relative stability. A sharp decrease in the product stability is observed at the MP2 level, which mainly depends on the level rather than on the geometry. For the modified catalyst, in fact, the HF/3-21G//B3P86/3-21G relative energy is −10.9 kcal/mol (vs −15.2 kcal/mol at the B3P86/3-21G level) when Rh is described by LANL1DZ, and −22.3 kcal/mol (vs −10.4 kcal/mol) when Rh is described by LANL2DZ. The MP2/3-21G//B3P86/3-21G relative energy, on the contrary, is 0.69 and −1.11 kcal/mol, respectively, when Rh is described by LANL1DZ and LANL2DZ. If geometry optimization at the MP2 level is performed, the relative stability of the products further decreases, becoming 2.9 kcal/mol (LANL1DZ) and −0.9 kcal/mol (LANL2DZ). An analogous trend is found using the unmodified catalyst (last column of the upper part of Table 1). This is in agreement with the findings in refs 4, 12, and 13b. Rocha and De Almeida, however, reported a similar trend already at the BP86/MIX level (see Table 1 of ref 13b), with $H-Rh(PH_3)_2CO$ as a catalyst. (MIX here stands for 6-31G* on P, O, and C; 3-21G on the olefin Hs; 3-21G plus three *p*-polarization functions on the H bonded to Rh; STO-3G on the phosphine Hs; and relativistic ECP and valence double-z basis set[21b] on Rh.) We repeated their calculations using BP86/MIX, optimizing the structures model-built according to Figure 1 of ref 13b, and obtained only slightly different results. [The linear product was −1.8 kcal/mol (−1.7 kcal/mol in ref 13b), i.e., more stable than the reactants (taken as zero), while the branched one was 0.6 kcal/mol (1.1 kcal/mol in ref 13b), i.e., less stable than the reactants.] It is worth noticing that the LANL2DZ description was still used for Rh, but the functions were probably contracted in a different way with respect to the original paper. What is more important, however, is that we found an additional number of minimum energy structures (shown in Figures 1S and 2S of the Supporting Information), which turned out to be even more favorable than those in ref 13b, both for the reactants and the products. For the reactants, in fact, the structure with the H bonded to Rh pointing away from the methyl substituent was just 0.24 kcal/mol more stable than the opposite one (REAC) described in ref 13b, whereas for the linear and branched products, the structures with the phosphines symmetrically located with respect to the CO group (geometries more consistent than PROD1 and PROD2 with TS1 and TS2 of ref 13b) were, respectively, −4.51 and −1.43 kcal/mol with respect to the new lowest energy minimum for the reactants. Of course, the wealth of structures is due to the presence of two different ligands in the modified catalyst, but this kind of problem could also be faced in the present study, though in a less dramatic way because we deal with CO ligands only. Consequently, the various possible adducts with the unmodified catalyst were considered.

(25) (a) Møller, C.; Plesset, M. S. *Phys. Rev.* **1934**, *46*, 618. (b) Pople, J. A.; Binkley, J. S.; Seeger, R. *Int. J. Quantum Chem.* **1976**, *10s*, 1. (c) Krishnan, R.; Frisch, M. J.; Pople, J. A. *J. Chem. Phys.* **1980**, *72*, 4244.

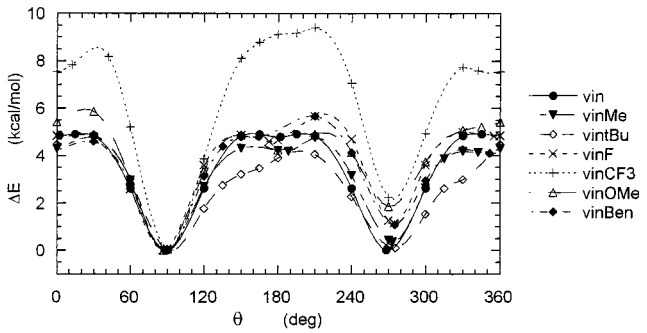

Figure 1. Potential energy profiles in the flexible rotor approximation computed at the B3P86/3-21G level for the rotation θ (see Scheme 2) of $H-Rh(CO)_3$ above the middle of the olefin double bond (see the legend, where vin = ethene, vinMe = propene, vintBu = 3,3-dimethylbutene, vinF = fluoroethene, $vinCF_3$ = 3,3,3,-trifluoropropene, vinOMe = vinylmethyl ether, vinBen = styrene).

The potential energy for the rotation θ of $H-Rh(CO)_3$ above the olefin C=C double bond in the complex of the reactants (R1; for the definition of θ, see Scheme 2, Reac, where $\theta = 0°$) has been considered in the flexible rotor approximation. In the curve for ethene, which is of course symmetric, shown in Figure 1 (solid line), there are two deep minima when the Rh−H bond is perpendicular (i.e. with θ either equal to 90° or 270°) to the C=C double bond, whereas there are two shallow local minima when the Rh−H bond is parallel to it ($\theta = 0°$, 180°). Morokuma et al.,[12a] in fact, dealing with ethylene, considered only two conformations: $\theta = 0°$ (**1a′**) and 90° (**1a** ≡ **1b** in our unmodified catalyst).

Depending on the electronic properties and on the steric hindrance of the substituent to the vinyl group (see Scheme 4), the shape of the curve and the barrier along it change somewhat (Figure 1). The minimum in all the cases is found about $\theta \approx 90°$ and the curves in the region 180−360° are shifted upward, raising thus the barrier and the bottom of the potential energy well. This effect is especially remarkable for 3,3,3-trifluoropropene with the highest barrier in the set (∼9 kcal/mol). On the contrary, in 3,3-dimethylbutene, where the fluorine atoms are replaced by methyl groups, the trend is more favorable than for ethene and just a small inflection in the region of $\theta \approx 180°$ or $\theta \approx 330°$ can be seen. Intermediate between 3,3-dimethylbutene and ethene is propene, whereas the effect of a fluorine atom is similar to that of a phenyl ring.

A slightly different behavior is found for vinylmethyl ether, because of the flexibility introduced by the presence of the ether O in the complex. The potential energy for the rotation about the $CH_3-O-C-C$ dihedral was examined in the flexible rotor approximation in the region $\theta \approx 90°$ (Figure 2a). There are two minima, the deepest one at $CH_3-O-C-C \approx 164°$ and the other at $CH_3-O-C-C \approx 0°$, separated by a barrier of ∼5 kcal/mol. In Figure 2b, the potential energy profile for either of the $CH_3-O-C-C$ values is displayed. When CH_3-

Downloaded by CARLI CONSORTIUM on June 29, 2009
Published on November 7, 2001 on http://pubs.acs.org | doi: 10.1021/om010721m

Scheme 4

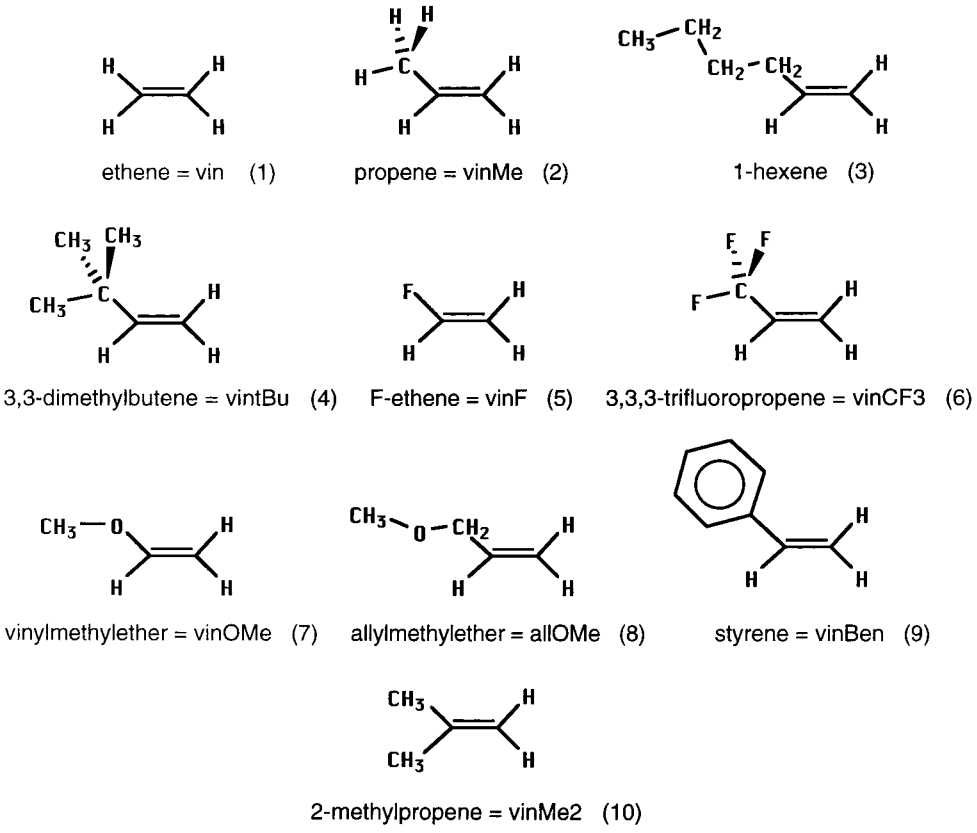

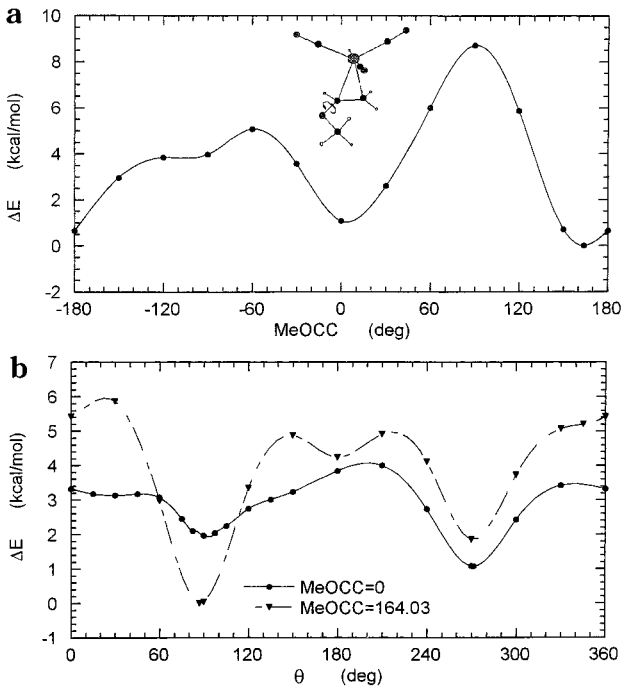

Figure 2. B3P86/3-21G potential energy profiles for vinylmethyl ether in the flexible rotor approximation (a) for the torsion Me−O−C=C and (b) for the rotation θ (same remarks as in Figure 1) at MeOCC = 0° (syn) or 164.03° (see the legend).

O−C−C ≈ 0°, the potential energy is smoother, suggesting that, when 120° ≤ θ ≤ 60°, CH_3−O−C−C might move from 0° to 164°. Because of this behavior, particular attention was paid to all the flexible structures for reactants, transition states, and products.

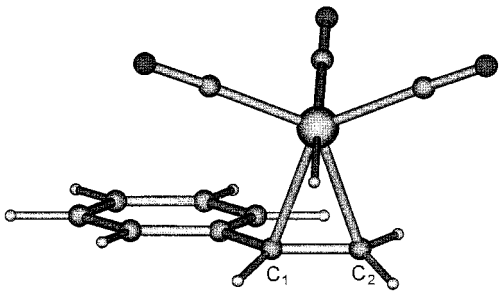

Figure 3. Lowest energy structure (E = −758.400 848 hartrees) of the styrene···H−Rh$(CO)_3$ complex at the B3P86/3-21G level; Rh···C_1 = 2.30 Å; Rh···C_2 = 2.27 Å.

Overview of the Mechanism. The PES's for the reaction mechanisms leading to the linear and branched aldehydes were then studied at the B3P86/3-21G level, using styrene as a model olefin. Rh···C_1/H···C_2 or Rh···C_2/H···C_1, respectively, were used as leading parameters for the branched or linear alkyl intermediate surface. The lowest energy minimum for the reactant adduct, obtained for $\theta \approx 90°$ (see Figure 1), is displayed in Figure 3: the Rh−H bond is located along the perpendicular to the side chain double bond above the half-plane containing vinyl hydrogens only. The apical CO group is, consequently, above the half-plane containing also the substituent (in this case a phenyl ring), while the CO groups forming the trigonal base are roughly in the same plane as the C_1=C_2 double bond.

The isopotential energy maps for the two pathways are displayed in Figure 4. Interestingly enough, the reactant arrangements (marked with a star in the upper left corner of the maps) to obtain the **b** ($\theta \approx 0°$) or **l** ($\theta \approx 180°$) aldehyde can easily be reached from the

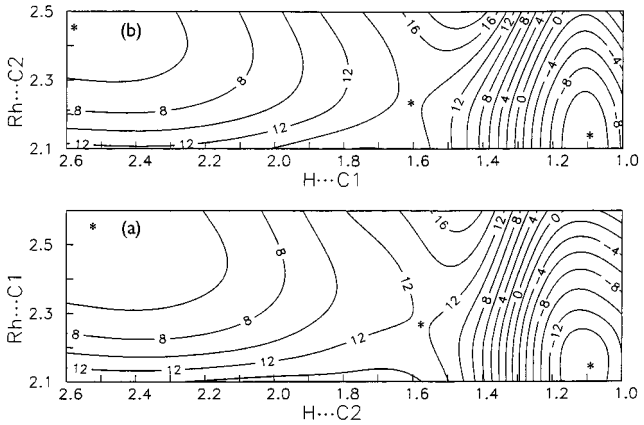

Figure 4. Potential energy surfaces computed at the B3P86/3-21G level for the hydride transfer from H−Rh-$(CO)_3$ to the vinyl group of styrene for the mechanisms leading to the (a) branched and (b) linear aldehydes. The locations of the reactant (R), product (P), and transition state (TS) adducts are marked with a star. Isopotential curves, up to 14 kcal/mol, are spaced by 2 kcal/mol. Distances are in Å.

minimum energy position reported in Figure 3: the relevant barriers are, in fact, just 4.1 and 4.9 kcal/mol, respectively. The general shape of the two surfaces is similar, though the PES for **l** is somewhat steeper than that for **b** on the reactant side (the reverse occurs on the product side). While the Rh···C separation decreases slightly, the hydride steadily approaches the other C atom. The transition state is reached in both cases for a C···H separation of about 1.6 Å. By examining the normal mode with imaginary frequency at the linear and branched TS, the largest displacement corresponds to the hydride, followed by the pyramidalization at both C_1 and C_2.

The accurate investigation of the PES carried out for two test cases allows one to gain an insight into the reaction mechanisms and to focus the attention only on the stationary points of the various surfaces from now on.

Structure and Energy of the Rh−Olefin Complexes. Several olefins have been considered besides ethene, which being symmetric is used as a reference, to elucidate the dependence of regioselectivity on the substrate electronic structure and properties. The substituents to the double bond can roughly be grouped into two classes: (1) R = alkyl and (2) R = phenyl, F, CF_3, OCH_3. The first type of substituents usually produces equal amounts of the aldehydic **b** and **l** isomers, while the second type gives rise to compounds such as styrene or other functionalized substrates, which favor branched aldehydes.[26] A vinylidenic substrate (Scheme 5), with R = R′ = CH_3, has also been taken into account.

Scheme 5

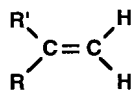

The B3P86 results are reported at the 3-21G and 6-31G* levels, respectively, in Tables 2 and 3, where the differential energies, such as $\Delta E^{\ddagger} = E_{TS} - E_{Reac}$, $\Delta E_{rel} = E_{Prod} - E_{Reac}$, $\Delta\Delta E^{\ddagger} = \Delta E^{\ddagger}$ (**b**) $- \Delta E^{\ddagger}$ (**l**), and $\Delta\Delta E_{rel} = \Delta E_{rel}$(**b**) $- \Delta E_{rel}$(**l**), are in kcal/mol. The reference energy (in hartrees) for each complex (E_{Reac}) is listed beside the substrate nickname (see Scheme 4). It is worth noting that for each structure a careful scan of the potential energy surface was carried out, to prevent the geometries from getting stuck in a local minimum. Some geometrical parameters optimized at the B3P86/6-31G* level are shown in Tables 4−6, while those related to the 3-21G basis set are reported in the Supporting Information (Tables IIIS−VS).

From a comparison of the values obtained with the two basis sets, it is apparent that there is a non-negligible difference in the relative energy, ΔE_{rel}, mainly for the second group of substrates. Conversely, the activation energy, $\Delta E^{\ddagger}$, is less basis set dependent especially for the path leading to the linear aldehydes. As an almost general rule the B3P86/6-31G* activation barriers are lower than the B3P86/3-21G ones for the compounds considered here, with the only exceptions being the vinylidenic substrate, particularly for the branched path, and of 3,3-dimethylbutene along the linear path, whose barriers, however, differ by ∼0.13 kcal/mol.

The activation barriers are plotted against each other for either the linear (regression coefficient, $r_{\mathbf{l}} = 0.994$) or branched ($r_{\mathbf{b}} = 0.952$) paths in Figure 5. The corresponding regression coefficients for the relative energies (plots not displayed) are comparable ($r_{\mathbf{b}} = 0.953$) or slightly worse ($r_{\mathbf{l}} = 0.799$).

Table 2. B3P86/3-21G Energetic Quantities[a] for Complexes between a Number of Substrates and an Unmodified Rhodium Catalyst (H−Rh(CO)$_3$), Optimized at That Level

		b		**l**		**b − l**	
substrate[b]	E_{Reac}[c]	$\Delta E^{\ddagger}$	ΔE_{rel}	$\Delta E^{\ddagger}$	ΔE_{rel}	$\Delta\Delta E^{\ddagger}$	$\Delta\Delta E_{rel}$
vin	−527.891 700	12.50	−11.09	12.50	−11.09		
vinMe	−567.143 002	12.07	−8.86	12.15	−9.77	−0.08	0.92
1-hexene	−684.890 205	11.81	−8.87	12.01	−9.33	−0.20	0.46
vintBu	−684.890 871	10.91	−8.64	9.68	−11.70	1.23	3.06
vinF	−626.723 362	13.64	−15.15	16.80	−15.30	−3.15	0.15
vinCF_3	−863.681 633	13.75	−16.66	17.05	−14.70	−3.29	−1.96
vinOMe	−642.072 631	12.51	−11.56	13.64	−11.02	−1.13	−0.54
allOMe	−681.319 601	13.56	−11.97	14.86	−17.22	−1.30	5.25
vinBen	−758.400 848	11.99	−16.25	14.39	−12.01	−2.39	−4.24
vinMe_2	−606.393 796	12.70	−7.25	11.49	−9.94	1.21	2.69

[a] For the ΔE (kcal/mol) definitions, see the text. [b] See Scheme 4 for structures. [c] Reference energy (E_{reac}) in hartrees.

Table 3. B3P86/6-31G* Energetic Quantities[a] for Complexes between a Number of Substrates and an Unmodified Rhodium Catalyst (H−Rh(CO)$_3$), Optimized at that Level

		b		**l**		**b − l**	
substrate[b]	E_{Reac}[c]	$\Delta E^{\ddagger}$	ΔE_{rel}	$\Delta E^{\ddagger}$	ΔE_{rel}	$\Delta\Delta E^{\ddagger}$	$\Delta\Delta E_{rel}$
vin	−530.189 427	12.46	−11.33	12.46	−11.33		
vinMe	−569.651 716	11.92	−8.62	12.06	−10.13	−0.14	1.51
1-hexene	−688.031 752	11.69	−8.52	11.69	−9.86	−0.01	1.35
vintBu	−688.028 482	10.78	−7.95	9.78	−11.55	1.00	3.60
vinF	−629.553 511	13.07	−13.98	15.36	−13.50	−2.29	−0.48
vinCF_3	−867.787 763	13.42	−14.01	15.77	−13.15	−2.35	−0.86
vinOMe	−644.996 062	12.26	−8.75	13.33	−8.72	−1.06	−0.03
allOMe	−684.451 290	12.73	−10.37	13.88	−13.27	−1.14	2.90
vinBen	−761.962 338	11.67	−13.79	13.99	−8.62	−2.31	−5.17
vinMe_2	−609.113 140	12.92	−5.71	11.56	−9.59	1.36	3.88

[a] For the ΔE (kcal/mol) definitions, see the text. [b] See Scheme 4 for structures. [c] Reference energy (E_{reac}) in hartrees.

(26) (a) Lazzaroni, R.; Settambolo, R.; Caiazzo, A. In *Rhodium Catalyzed Hydroformylation*, van Leeuwen, P. W. N. M., Claver, C., Eds.; Kluwer: Dordrecht, 2000; Chapter 2. (b) Lazzaroni, R.; Pertici, P.; Bertozzi, S.; Fabrizi, G. *J. Mol. Catal.* **1990**, *58*, 75.

Downloaded by CARLI CONSORTIUM on June 29, 2009
Published on November 7, 2001 on http://pubs.acs.org | doi: 10.1021/om010721m

Table 4. B3P86/6-31G* Geometric Parameters[a] for the Reactant Complexes between a Number of Substrates and an Unmodified Rhodium Catalyst [H−Rh(CO)$_3$]

substrate	RhC_n	RhH	HC_n	RhC_{ax}	$\angle C_{ax}RhH$	RhC_{eq}	C_1C_2
vin	2.254	1.594	2.614	1.975	177.67	1.943	1.393
vinMe	2.266	1.596	2.630	1.970	178.60	1.943	1.391
	2.299		2.645			1.939	
1-hexene	2.252	1.596	2.610	1.969	178.20	1.940	1.394
	2.300		2.643			1.945	
vintBu	2.280	1.598	2.633	1.966	178.04	1.940	1.388
	2.354		2.636			1.935	
vinF	2.237	1.595	2.616	1.980	177.34	1.942	1.390
	2.237		2.640			1.959	
$vinCF_3$	2.202	1.591	2.581	1.991	178.63	1.951	1.407
	2.190		2.522			1.958	
vinOMe	2.280	1.598	2.665	1.970	177.60	1.945	1.385
	2.363		2.729			1.928	
allOMe	2.244	1.595	2.616	1.985	178.70	1.946	1.396
	2.256		2.593			1.939	
vinBen	2.263	1.596	2.631	1.976	179.05	1.942	1.393
	2.325		2.677			1.938	
$vinMe_2$	2.294	1.596	2.661	1.966	178.84	1.933	1.387
	2.394		2.750			1.934	

[a] Distances in Å, angles in degrees; in the entries where C_n appears, the lower line refers to the substituted olefin C.

Table 5. B3P86/6-31G* Geometric Parameters[a] for the Transition States between a Number of Substrates and an Unmodified Rhodium Catalyst [H−Rh(CO)$_3$]

Linear

substrate	RhC_2	RhH	HC_1	RhC_{ap}	$\angle C_{ap}RhH$	RhC_b	C_1C_2
vin	2.262	1.654	1.623	1.987	88.61	1.923/1.922	1.402
vinMe	2.254	1.656	1.588	1.982	89.01	1.925/1.918	1.407
1-hexene	2.254	1.652	1.617	1.983	89.14	1.922/1.920	1.406
vintBu	2.245	1.646	1.677	2.000	89.83	1.929/1.912	1.406
vinF	2.227	1.660	1.618	2.010	90.07	1.922/1.917	1.404
$vinCF_3$	2.203	1.641	1.645	2.000	91.47	1.943/1.925	1.415
vinOMe	2.197	1.677	1.604	2.016	91.99	1.921/1.915	1.425
allOMe	2.257	1.661	1.561	1.979	87.91	1.931/1.911	1.407
vinBen	2.228	1.657	1.636	1.998	89.78	1.924/1.919	1.414
$vinMe_2$	2.243	1.655	1.590	1.988	89.44	1.921/1.918	1.413

Branched

substrate	RhC_1	RhH	HC_2	RhC_{ap}	$\angle C_{ap}RhH$	RhC_b	C_1C_2
vinMe	2.276	1.649	1.635	1.987	89.64	1.930/1.922	1.406
1-hexene	2.289	1.647	1.636	1.983	89.00	1.929/1.923	1.405
vintBu	2.297	1.649	1.611	1.978	89.46	1.930/1.925	1.408
vinF	2.229	1.644	1.674	1.993	89.11	1.936/1.931	1.401
$vinCF_3$	2.217	1.643	1.678	2.003	88.20	1.935/1.922	1.407
vinOMe	2.337	1.648	1.626	1.972	87.93	1.929/1.929	1.400
allOMe	2.256	1.643	1.660	1.994	87.88	1.932/1.919	1.405
vinBen	2.327	1.655	1.596	1.977	88.39	1.926/1.925	1.408
$vinMe_2$	2.331	1.659	1.545	1.961	87.87	1.940/1.918	1.413

[a] Distances in Å, angles in degrees.

Table 6. B3P86/6-31G* Geometric Parameters[a] for the Product Intermediates between a Number of Substrates and an Unmodified Rhodium Catalyst [H−Rh(CO)$_3$]

Linear

substrate	RhC_2	RhC_{ax}	$\angle RhC_2C_1$	RhC_{eq}	C_1C_2
vin	2.149	1.941	106.36	1.923	1.524
vinMe	2.151	1.939	107.79	1.924/1.922	1.526
1-hexene	2.160	1.938	110.46	1.926/1.921	1.526
vintBu	2.149	1.946	113.50	1.927/1.915	1.529
vinF	2.147	1.932	110.86	1.948/1.914	1.508
$vinCF_3$	2.148	1.939	110.97	1.928/1.919	1.525
vinOMe	2.149	1.931	110.41	1.949/1.912	1.513
allOMe	2.136	1.948	106.76	1.916/1.912	1.525
vinBen	2.153	1.939	107.79	1.931/1.915	1.531
$vinMe_2$	2.159	1.938	111.59	1.927/1.921	1.530

Branched

substrate	RhC_1	RhC_{ap}	$\angle RhC_1C_2$	RhC_{eq}	C_1C_2
vinMe	2.160	1.949	116.09	1.928/1.918	1.521
1-hexene	2.171	1.948	114.67	1.926/1.918	1.523
vintBu	2.194	1.939	112.68	1.927/1.923	1.527
vinF	2.105	1.967	119.38	1.938/1.915	1.508
$vinCF_3$	2.159	1.930	109.17	1.943/1.925	1.526
vinOMe	2.150	1.965	115.84	1.934/1.917	1.513
allOMe	2.167	1.930	111.01	1.959/1.913	1.525
vinBen	2.139	1.949	121.16	1.925/1.919	1.513
$vinMe_2$	2.164	1.964	114.29	1.920/1.920	1.522

[a] Distances in Å, angles in degrees.

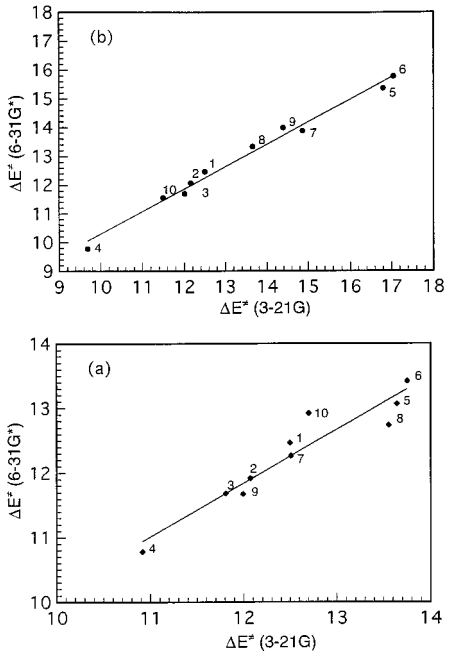

Figure 5. B3P86/3-21G vs B3P86/6-31G* activation energies ($\Delta E^{\ddagger}$, kcal/mol) for a number of substrates (see Scheme 4) along the (a) branched and (b) linear paths.

Single point MP2/6-31G* calculations, carried out on the B3P86/6-31G* geometries for ethene, propene, and F-ethene, brought out a sharp increase in ΔE_{rel} with respect to the values obtained at the B3P86/6-31G* level, while the barriers, i.e., $\Delta E^{\ddagger}$, were roughly conserved.

To understand the origin of this behavior (already mentioned above when discussing the results reported in Table 1), MP2/6-31G* geometry optimizations were carried out on those systems. Interestingly, geometries and energies did not considerably change after optimization, indicating that the structures were already close to MP2 minima. A major incidence of the dispersion energy on reactants and transition states, by lowering their energies with respect to the products, is likely to be responsible for the observed decrease in the product stabilities. The product structures are, in fact, characterized by well-separated arrangements of the catalyst with respect to the hydrocarbon backbone (along the branched path as well), in contrast to reactants and TS that feature the transition metal bridged between the two olefinic carbons.

Typical geometries of reactants, (linear and branched) TS, and products are shown in Figure 6, where the F-ethene insertion into the Rh−H bond is displayed. The structural change from TBP (reactants) to SP (transition state) occurs via the Berry pseudorotation mechanism,

Downloaded by CARLI CONSORTIUM on June 29, 2009
Published on November 7, 2001 on http://pubs.acs.org | doi: 10.1021/om010721m

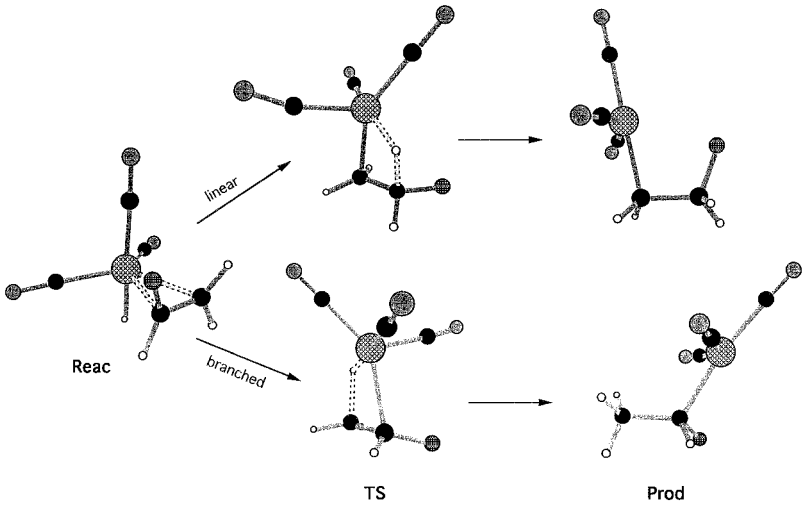

Figure 6. B3P86/3-21G equilibrium structures along the linear and branched paths for F-ethene + H−Rh(CO)$_3$.

Downloaded by CARLI CONSORTIUM on June 29, 2009
Published on November 7, 2001 on http://pubs.acs.org | doi: 10.1021/om010721m

Scheme 6

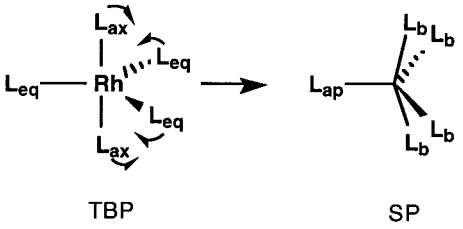

which brings the axial ligands and two of the equatorial ones to a basal position, causing the third equatorial ligand to become apical (see Scheme 6), followed by a similar rearrangement leading to the products. Notice that the apical ligand in the linear TS of Figure 6 is located at the left side as in Scheme 6, whereas in the branched TS it is located at the right side, because we preferred to keep the olefin in a similar orientation along both paths.

There are steady regularities within the B3P86/6-31G* values of bond lengths and angles in the whole series, as can be derived from a perusal of Tables 4−6, as well as from Tables IIIS−VS (B3P86/3-21G values reported in parentheses), with limited exceptions for the F-containing compounds.

In the reactants (1) the Rh−C(olefin) separations are slightly longer when C bears a substituent than when it bears hydrogens; (2) the Rh−H distances, in the interval 1.591−1.598 Å (1.584−1.593 Å), are very close to the X-ray value of 1.60 ± 0.12 Å, determined, however, in TBP H−Rh(CO)(PH$_3$)$_3$;[27] (3) the Rh−C$_{ax}$ distances, ranging from 1.966 to 1.991 Å (1.968−1.998 Å), are longer than the corresponding Rh−C$_{eq}$ distances, 1.928−1.958 Å (1.936−1.976 Å). This effect, the well-known trans influence, is due to the axial position of H in all the reactant structures considered here; (4) the bond angles between the axial ligands, in the range 177.34−179.05° (176.63−179.43°), are very close to 180°.

In the transition states (1) the Rh−C$_n$ separations are slightly longer for branched than linear intermediates, probably because of the proximity to Rh of the substituent in the branched TS; (2) the Rh−H and H−C$_n$ distances become comparable, as expected; (3) the bond angles between the apical C and the basal groups are all below 120° and close to 100°, while the smallest value, slightly lower than 90° in TSB and about 90° in TSL, is found for H; (4) the Rh−C$_{ap}$ distances, ranging from 1.961 to 2.016 Å (1.961−2.015 Å), are still longer than the corresponding Rh−C$_b$ distances, 1.911−1.943 Å (1.909−1.948 Å).

The geometrical features of the products are affected by the Rh−substituent interactions: the substituent moiety, in fact, now free to rotate about the C−C single bond, moves to face Rh (as shown in Figure 6, linear path product). This occurs also for styrene and the methoxy groups. In the case of allylmethyl ether, the increased flexibility of the substituent to the double bond allows the methoxy O to approach one of the carbonyl C also in the branched product. Consequently, a remarkable difference in the Rh−C$_{eq}$ bond lengths can be observed. At the 3-21G level, probably due to the lack of polarization functions, the Rh−C$_2$−C$_1$ bond angle sharply decreases in the linear products of the reaction of H−Rh(CO)$_3$ with styrene, vinylmethyl ether, and F-ethene, allowing Rh to approach the substituent.

Regioselectivity

Experimental Regioisomeric Ratio Determined for the Isomeric Aldehydes. To obtain a consistent set of experimental results for most of the compounds considered in the theoretical calculations, hydroformylation of the vinyl substrates (R−CH=CH$_2$) 2−4 and 7−10 has been carried out at room temperature in the presence of Rh$_4$(CO)$_{12}$ as catalyst precursor at 80 atm CO/H$_2$ (1:1) in an apolar solvent. The substituent R at the vinyl moiety can thus be a linear alkyl (2, 3), a branched alkyl (4), or a phenyl ring (9). Alkoxy-substituted vinyl (7) and allyl (8) substrates have also been examined as well as a 1,1-disubstituted olefin (10). The results are reported in Table 7.

In the experimental conditions adopted (also shown in Table 7), the substrate conversion is more than 99% in 16−24 h, aliphatic substrates reacting faster than styrene or vinyl ethers. Only in the case of 2-methyl-2-propene (10) was the reaction carried out at 80 °C, because this substrate is unreactive at room temperature. The experimental regioisomeric ratio **b**:**l** strictly depends on the substrate structure. The branched

(27) La Placa, S. J.; Ibers, J. A. *Acta Crystallogr.* **1965**, *18*, 511.

Table 7. Rhodium-Catalyzed Hydroformylation of Vinyl Substrates in the Presence of $Rh_4(CO)_{12}$ as Catalyst Precursor[a]

Substrate	Reaction times (h)	Conversion[b] (%)	b:l[b]
2 vinMe	15	70	50:50
3 1-hexene	18	60	48:52
	24	>99	48:52
4 vintBu	6	23	10:90
7 vinOMe	7	30	83:17
	15	60	83:17
8 allOMe	16	70	70:30
9 vinBen	7	60	98:2
	15	100	98:2
10[c] $vinMe_2$	2	100	1:99

[a] Reaction conditions: 5 mmol of substrate, 5 mL of benzene, 12.5 μmol of $Rh_4(CO)_{12}$; autoclave volume 25 mL; 25 °C; 80 atm of total pressure (CO/H_2 = 1:1). [b] Determined via GC on the total reaction products using an internal standard; aldehyde selectivity > 99%. [c] Temperature 80 °C.

Table 8. Regioselectivity (b:l) for the Complexes with Unmodified Rhodium Catalysts Obtained from the B3P86/3-21G and 6-31G* Activation Energies ($\Delta E^{\ddagger}$), Corrected for the Zero Point Energy [Δ(E+ZPE)‡], from the Activation Enthalpies ($\Delta H^{\ddagger}$), and from the Activation Free Energy ($\Delta G^{\ddagger}$); the Experimental Ratios Are Also Shown for Comparison

	b:l ($\Delta E^{\ddagger}$)		b:l [Δ(E+ZPE)‡]		b:l ($\Delta H^{\ddagger}$)		b:l ($\Delta G^{\ddagger}$)		
substrate	3-21G	6-31G*	3-21G	6-31G*	3-21G	6-31G*	3-21G	6-31G*	expl b:l
vinMe	53:47	56:44	63:37	63:37	60:40	62:38	64:36	59:41	50:50
1-hexene	58:42	50:50	58:42	49:51	61:39	51:49	13:87	10:90	48:52
vintBu	11:89	15:85	10:90	13:87	11:89	14:86	8:92	9:91	10:90
vinF	100:0	98:2	100:0	98:2	99:1	98:2	99:1	97:3	100:0[a]
$vinCF_3$	100:0	98:2	99:1	98:2	99:1	98:2	99:1	97:3	97:3[a]
vinOMe	87:13	86:14	91:9	90:10	88:12	86:14	96:4	95:5	83:17
allOMe	90:10	87:13	93:7	90:10	92:8	89:11	95:5	88:12	70:30
vinBen	98:2	98:2	98:2	97:3	98:2	97:3	98:2	98:2	98:2
$vinMe_2$	11:89	9:91	17:83	8:92	4:96	8:92	10:90	10:90	1:99

[a] From ref 28.

aldehydic isomer strongly prevails in the case of styrene (9) and methylvinyl ether (7), while it is still quite predominant in the case of methylallyl ether (8). The amounts of aldehydic isomers are equivalent in the case of vinyl substrates bearing a linear alkyl group (2, 3), while linear aldehyde is the prevailing or exclusive product in the case of a branched alkyl substituent (4) or in the case of an 1,1-disubstituted olefin (10). It is worthy to remark that an almost complete regioselectivity has been reported for fluorinated vinyl substrates (perfluoro ethene, trifluoromethyl propene).[28] Experiments carried out at different substrate conversions and rhodium concentrations show that regioselectivity is not influenced by these latter parameters.

Theoretical Regioisomeric Ratio Evaluated in the Alkyl−Rhodium Intermediate Formation. The regioselectivity can be estimated making use of a formula, successfully used previously,[14] that takes into account only the relative energies of the **b** and **l** transition states:

$$\mathbf{b}:\mathbf{l} = k_{\mathbf{b}}:k_{\mathbf{l}} = e^{-\Delta G_{\mathbf{b}}^{\ddagger}/RT}:e^{-\Delta G_{\mathbf{l}}^{\ddagger}/RT} = e^{-\Delta\Delta G^{\ddagger}/RT} \approx e^{-\Delta\Delta E^{\ddagger}/RT}$$

This assumption is viable because the olefin insertion was demonstrated to occur irreversibly and without subsequent changes in the **b**:**l** distribution,[1a,7,8d] i.e., [**b**] + [**l**] = $[TS_{\mathbf{b}}] + [TS_{\mathbf{l}}] = 1$. An evaluation of the isomeric ratios for the various compounds can thus be performed, by using the transition state barriers ($\Delta E^{\ddagger}$) determined thus far. The values obtained, reported in Table 8, are to be compared to the proper experimental results, mentioned above.

The agreement between computed and experimental data is in general very good. It should be noted, however, that ratios close to 50:50 are much more sensitive to small energy differences than those largely

(28) Ojima, I. *Chem. Rev.* **1988**, *88*, 1011.

Downloaded by CARLI CONSORTIUM on June 29, 2009
Published on November 7, 2001 on http://pubs.acs.org | doi: 10.1021/om010721m

Downloaded by CARLI CONSORTIUM on June 29, 2009
Published on November 7, 2001 on http://pubs.acs.org | doi: 10.1021/om010721m

favoring an isomer over the other (i.e., 100:0 or 0:100). Therefore, the use of internal energy, corrected for zero point energy or not, enthalpy, or free energy does not make any change for the regioselectivity of vinF, vinCF_3, vinOMe, allOMe, and vinBen, whereas those for vinMe and 1-hexene are appreciably affected. An analogous effect on regioselectivity is produced by the basis set.

In the case of substrates such as propene and 1-hexene, the contribution of hindered rotations of the methyl group or of the aliphatic chain should be included in the free energy calculations.[29] This term in fact is especially important for transition states. The free energy gap between the TS of the **b** and **l** isomers is actually very limited; consequently, even negligibly small differences between **b** and **l** hindered rotations might produce a change of sign in the relative stability of the two species. On the other hand, unfortunately, each hindered rotation is strictly coupled in the low-frequency normal modes to real vibrations, whose contribution to the entropy thus cannot be completely discarded. This is to point out that sensitive variations in the free energy derive from assigning different (within a sensible choice) percentages, respectively, to vibrations and hindered rotations. Very small amounts can move the ratio in such a way as to favor either form, since a few tenths of a kcal/mol are sufficient to reverse the stability order. Analogously, the use of scaling factors, even though very close to 1, for the frequencies, can affect the results.

However, since our aim is not to reproduce experimental results but to clarify whether computational methods allow us to predict the regioselectivity, we can well affirm that transition state free energy differences lower than 0.5 kcal/mol indicate no preference for either compound.

$VinMe_2$ and vintBu, though, belonging to the first type of substituents (aliphatic hydrocarbons), show a different behavior with respect to vinMe and 1-hexene. This probably occurs because of the steric hindrance due to the methyl groups in close proximity to one of the catalyst CO in the TS leading to the branched aldehyde, which is relieved in the linear intermediate.

The difference in the relative energy for the isomeric product intermediates, used to evaluate the regioisomeric ratio in connection to modified catalysts,[13b] in the present set of substrates only occasionally produces results in agreement with the experimental ones. On average, actually, the results are rather discordant (see, for instance, vinMe and 1-hexene), while for vinF and the methoxy-substituted olefins the ratios turn out to be completely wrong.

Conclusions

The above findings clearly show that the regioisomeric ratio between the branched and linear aldehydes obtained in the hydroformylation of vinyl substrates of different structure is very similar to the regioisomeric ratio theoretically evaluated for branched and linear alkyl−metal transition state intermediates. The branched isomer strongly prevails when a polarizable or electron-withdrawing group is bonded to the vinyl moiety, whereas steric factors definitely favor the linear isomer. The same amount of linear and branched isomers is obtained in the case of normal alkyl substituents.

Our theoretical investigation confirms the hypothesis, repeatedly put forward, that under mild conditions the regioselectivity of the hydroformylation reaction originates at the alkyl formation step.

The use of unmodified rhodium catalysts, such as H−$Rh(CO)_3$, brings out some peculiar features of the complexes obtained after the olefin insertion into the Rh−H bond. In particular, at the B3P86/3-21G LANL2DZ level, using ethene as a model olefin, (1) the trigonal-bipyramidal structures with both olefin and H in equatorial position are not local minima, in contrast to what happened when a phosphine group was present; and (2) geometry optimizations at the TS allow one to obtain structures with an equatorial H which, anyway, are square planar.

Calculations carried out for comparison at different levels with modified catalysts (bearing one phosphine group) were sharply influenced by the use of LANL1DZ in place of LANL2DZ.

The B3P86/3-21G potential energy surfaces for the reaction mechanisms leading to the linear and branched alkyl intermediates, using styrene as a model olefin, are similar and show barriers much lower than that found for ethene with modified catalysts. The reactant arrangements on each surface can be reached from the $\theta \approx 90°$ minimum energy position for the complex, because the barriers are ∼4−5 kcal/mol at most.

MP2/6-31G* geometry optimizations do not considerably affect geometries and energies; conversely, when correlation corrected, the product stabilities sharply decrease, due to a dispersion energy incidence higher on reactants and transition states than on products.

The internal geometries of the reactants are fairly well conserved at both the B3P86/6-31G* and 3-21G levels for the various substituents. The $Rh-C_{ax}$ distances are longer than the $Rh-C_{eq}$ ones for the trans influence effect of the axial H. More sensitive are the variations for the transition states, with appreciable differences between branched and linear structures, while in the product intermediates the interactions between Rh and the substituent prevail, especially when the substituent is an electron-donating group, such as F, OCH_3, or phenyl.

As far as the regioselectivity is concerned, the theoretical ratio derived from the relative energies of the **b** and **l** transition states is fairly comparable to the experimental results, either determined in this work, making use of analogous reaction conditions in hydrocarbon solvents, or taken from the literature. When there is no clear-cut prevalence of an isomer over the other, as in the case of propene and 1-hexene, the ratios are very sensitive to small energy differences. They thus seem to critically depend on the computational method accuracy and level. Due to the difficulty of discriminating between real vibrations and hindered rotations, it is advisable to use either the internal energies, corrected or not for the zero point energy, or the enthalpies. Even without resorting to the time-consuming calculations requested to compute vibrational frequencies, in fact, a satisfactory value for regioselectivity can be derived from internal energies alone, when a sensible TS structure is obtained. It is worth pointing

(29) (a) Truhlar, D. G. *J. Comput. Chem.* **1991**, *12*, 266. (b) Ayala, P. Y.; Schlegel, H. B. *J. Chem. Phys.* **1998**, *108*, 2314.

out, in addition, that for predictive purposes transition states that differ by less than 0.5 kcal/mol cannot indicate a sharp preference for either compound.

The steric hindrance in 2-methylpropene and 3,3-dimethylbutene, which is higher than in propene and 1-hexene (belonging to the same class of substrates), is responsible for shifting the ratio toward the linear intermediate, because in that arrangement the groups can stay further apart.

Acknowledgment. The experimental work was supported by the Ministero dell'Università e della Ricerca Scientifica e Tecnologica (MURST, Roma), Programmi di Ricerca di rilevante interesse nazionale (2000-2001).

Supporting Information Available: This material is available free of charge via the Internet at http://pubs.acs.org.

OM010721M

Downloaded by CARLI CONSORTIUM on June 29, 2009
Published on November 7, 2001 on http://pubs.acs.org | doi: 10.1021/om010721m